Article

Facile Fabrication of Ag–Pd Bimetallic Nanoparticles in Ultrathin TiO-Gel Films: Nanoparticle Morphology and Catalytic Activity

Junhui He, Izumi Ichinose, Toyoki Kunitake, Aiko Nakao, Yukihide Shiraishi, and Naoki Toshima

J. Am. Chem. Soc., **2003**, 125 (36), 11034-11040• DOI: 10.1021/ja035970b • Publication Date (Web): 13 August 2003

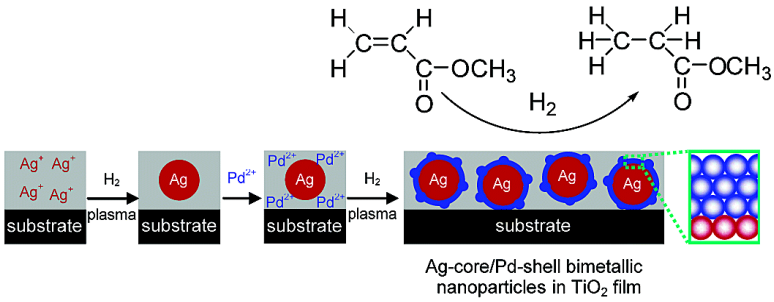

More About This Article

Additional resources and features associated with this article are available within the HTML version:

- Supporting Information
- Links to the 20 articles that cite this article, as of the time of this article download
- Access to high resolution figures
- Links to articles and content related to this article
- Copyright permission to reproduce figures and/or text from this article

View the Full Text HTML

J|A|C|S
ARTICLES
Published on Web 08/13/2003

Facile Fabrication of Ag−Pd Bimetallic Nanoparticles in Ultrathin TiO_2-Gel Films: Nanoparticle Morphology and Catalytic Activity

Junhui He,[†] Izumi Ichinose,[†] Toyoki Kunitake,*[,†] Aiko Nakao,[‡] Yukihide Shiraishi,[§] and Naoki Toshima[§]

Contribution from the Frontier Research System and Surface Science Division, The Institute of Physical and Chemical Research (RIKEN), 2-1 Hirosawa, Wako, Saitama 351-0198, and the Department of Materials Science and Environmental Engineering, Tokyo University of Science, Yamaguchi, Onoda, Yamaguchi 756-0884, Japan

Received May 6, 2003; E-mail: kunitake@ruby.ocn.ne.jp

Abstract: Ag−Pd bimetallic nanoparticles were prepared directly in ultrathin TiO_2-gel films by a stepwise ion-exchange/reduction approach. Ion-exchange sites were created in ultrathin films using Mg^{2+} ions as template. Ag^+ ion was then incorporated by ion exchange, and converted into metallic nanoparticles by low-temperature H_2 plasma, regenerating ion-exchange sites. The same procedure was then carried out for Pd^{2+} ion, producing Pd-on-Ag bimetallic nanoparticles, as TEM observation and plasmon resonance absorption indicate. By contrast, reversed metal incorporation procedure appeared to give a mixture of individual Ag and Pd nanoparticles, as confirmed by TEM, absorption spectroscopy and X-ray photoelectron spectroscopy. For hydrogenation of methyl acrylate, the catalytic activity of the Pd-on-Ag nanoparticle is 367 times as large as that of commercial Pd black and 1.6 times as large as that of Pd monometallic nanoparticle. The outstanding catalytic activity was explicable by the large fraction of the surface-exposed Pd atoms. The formation process of the bimetallic nanoparticle and their general morphological feature are discussed.

Introduction

Nanoparticles of metals and semiconductors are known to have unique features, such as surface plasmon absorption, improved magnetic property, high reactivity and enhanced catalytic activity, due to their small sizes and extremely large surface areas.[1−4] These features may be enhanced, modified or suppressed in the case of bimetallic and multi-metallic nanoparticles, because of inter-metallic interactions arising from their constitutional and morphological combinations. Totally new functions may be created by overcoming disadvantages of single component nanoparticles. Unique features expected for multi-metallic nanoparticles may include: (1) physical and chemical interactions among different atoms and phases that lead to novel functions; (2) altered miscibility and interactions unique to nanometer dimension (macroscopic phase property may not apply); and (3) morphological variations that are related to new properties.

As specific examples, gold−palladium (1:4) and platinum−palladium (1:4) core−shell nanoparticles show higher catalytic activities than the corresponding mixture of the monometallic nanoparticles for selective hydrogenation of cycloocta-1,3-diene to cyclooctene[5] and for hydrogenation of 4-pentenoic acid,[6] respectively. A Ni−Pd nanoparticle alloy reveals a composition-dependent catalytic activity, and the highest activity is achieved for a bimetallic nanocluster with a molar ratio of Ni:Pd = 2:3.[7] Very recently, dendrimer-encapsulated Pd−Pt nanoparticles were synthesized to give an enhanced catalytic activity for hydrogenation of allyl alcohol compared with physical mixtures of monometallic nanoparticles.[8] Another type of the example is monodisperse Fe−Pt nanoparticles and their assemblies (superlattices) that show high room-temperature magnetic susceptibility.[9] Morphological details of these bimetallic nanoparticles have not been made clear.

Both of the simultaneous and successive procedures have been used for preparation of bimetallic nanoparticles that are protected by surfactants or polymers in solution.[10] In practical applications,

[†] Frontier Research System, RIKEN.
[‡] Surface Science Division, RIKEN.
[§] Tokyo University of Science.

(1) Schmid, G. *Chem. Rev.* **1992**, *92*, 1709−1727.
(2) Schmid, G.; Hornyak, G. L. *Curr. Opinion Solid State Mater. Sci.* **1997**, *2*, 204−212.
(3) Pileni, M. P. In *Metal Nanoparticles: Synthesis, Characterization, and Applications*; Feldheim, D. L., Foss, C. A., Jr., Eds.; Marcel Dekker: New York, 2001, pp 207−236.
(4) (a) Toshima, N. In *Nanoscale Materials*; Liz-Marzán, L. M., Kamat, P., Eds.; Kluwer: Norwell, MA, 2003, pp 79−96; b) Toshima, N.; Yonezawa, T. *New J. Chem.* **1998**, *22*, 1179−1201.
(5) (a) Toshima, N.; Harada, M.; Yamazaki, Y.; Asakura, K. *J. Phys. Chem.* **1992**, *96*, 9927−9933; (b) Toshima, N.; Yonezawa, T.; Kushihashi, K. *J. Chem. Soc., Faraday Trans.* **1993**, *89*, 2537−2543.
(6) Mizukoshi, Y.; Fujimoto, T.; Nagata, Y.; Oshima, R.; Maeda, Y. *J. Phys. Chem. B* **2000**, *104*, 6028−6032.
(7) Lu, P.; Teranishi, T.; Asakura, K.; Miyake, M.; Toshima, N. *J. Phys. Chem. B* **1999**, *103*, 9673−9682.
(8) Scott, R. W. J.; Datye, A. K.; Crooks, R. M. *J. Am. Chem. Soc.* **2003**, *125*, 3708−3709.
(9) Sun, S.; Murray, C. B.; Weller, D.; Folks, L.; Moser, A. *Science* **2000**, *287*, 1989−1992.

10.1021/ja035970b CCC: $25.00

Scheme 1. Template Approach to the Incorporation of a Noble Metal Ion into TiO_2 Ultrathin Films and Nanoparticle Formation.

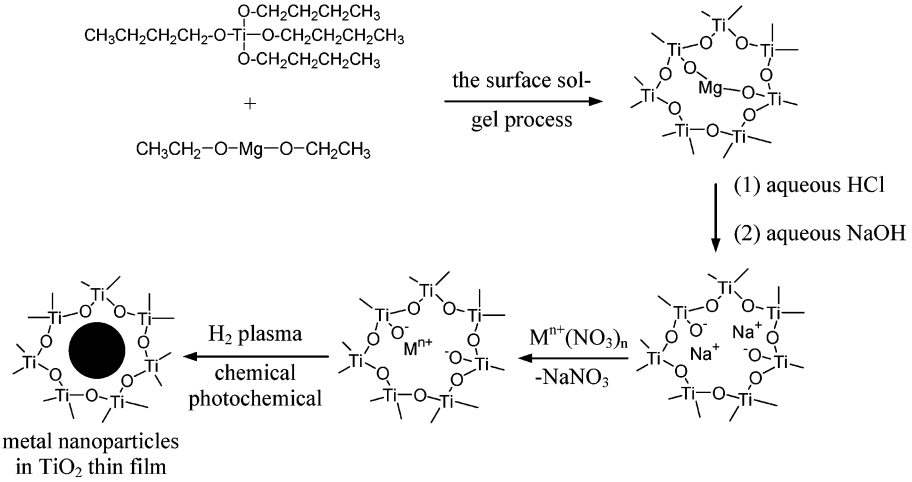

it is often required to immobilize these nanoparticles on solid supports. Several fabrication techniques have been reported for monometallic nanoparticles embedded in solid matrixes, including ion implantation,[11] sputtering,[12] sol−gel process/spin-coating,[13] and alternate layer-by-layer assembly.[14,15] However, convenient, in-situ preparation in solid matrixes is not known in the case of bimetallic nanoparticles.

Recently we developed a novel ion-exchange method for incorporation of metal ions into nanoporous metal oxide thin films (see Scheme 1).[16] Such noble metal ions were readily converted to monometallic nanoparticles in the thin film matrix by photoreduction, by chemical reduction, or by low-temperature H_2 plasma.[17] In a separate study, the Ag nanoparticle thus prepared was readily converted to the corresponding metal oxide nanoparticle by O_2 plasma, and repeated treatments by alternate H_2 and O_2 plasma resulted in monodisperse Ag and Ag oxide nanoparticles, respectively.[18] It is important to extend such simple procedures to bimetallic systems, because facile preparation of bimetallic and multimetallic nanoparticles is urgently needed for new nano-electronic and nano-magnetic materials and for high-efficiency fuel cells. In this paper, we demonstrate that this is in fact possible, and discuss morphology and catalytic property in the case of Pd−Ag bimetallic nanoparticles.

Experimental Section

A mixture of $Mg(O\text{-}Et)_2$ (10 mM) and $Ti(O\text{-}n\text{Bu})_4$ (100 mM) in 2-ethoxyethanol was used commonly for film assembly unless otherwise specified. A quartz plate was cleaned with concentrated sulfuric acid (96%), followed by treatment with 1 wt % ethanolic KOH (ethanol/water = 3:2, v/v). After rinsing in ion-exchanged water and drying with N_2 flushing, the plate was immersed in the precursor solution at room temperature for 10 min, followed by rinsing with toluene for 1 min to remove the physisorbed species, drying with N_2 and hydrolysis in air. Usually, 8 cycles of this procedure were repeated and the film thickness was estimated to be ca. 20 nm from QCM mass decrease.[16] To remove Mg^{2+} ions, the thin film was immersed in aqueous HCl of pH 4 for 20 min, rinsed with pure water for 2 min and dried with nitrogen gas. It was then treated with aqueous NaOH (pH 10) for 20 min, followed by rinsing in pure water for 2 min and drying with nitrogen gas. The film on a quartz plate was then immersed in aqueous $AgNO_3$ or $Pd(NO_3)_2$ (10 mM) for 4 h, rinsed with pure water for 1 min and dried by flushing nitrogen gas. The prepared film was then exposed to H_2 plasma. The same procedure was used for introducing the second metal (Pd or Ag). H_2 plasma treatment was carried out on a PE−2000 Plasma Etcher (South Bay Technology, USA). A pressure regulated flow rate of 0.02 MPa was set on the H_2 gas cylinder and the plasma chamber was evacuated to ca. 80 mTorr before introduction of H_2 gas. The operating pressure was regulated at ca. 180 mTorr. The forward power was set at 10 w unless otherwise indicated, while the reflected power was optimized. N_2 gas at 2.5 L/min was introduced into the pump for safety purpose.

UV−visible absorption spectra were recorded with a quartz plate as the reference on a Shimadzu UV-3100PC UV−vis−NIR scanning spectrophotometer. X-ray photoelectron spectroscopy (XPS) measurements were carried out on ESCALAB 250 (VG) using Al Kα (1486.6 eV) radiation. The applied power was operated at 15 kV and 20 mA. The base pressure in the analysis chamber was less than 10^{-8} Pa. Smoothing, background removal and peak fitting were carried out with a VG analysis software package, ECLIPS. All of the peaks were corrected with C 1s (285 eV) as the reference. Transmission electron microscopy (TEM) observations were carried out on a JEOL JEM-2000EX transmission electron microscope. Histogram, mean diameter and standard deviation were obtained by sampling 100 metal nanoparticles in TEM images of 3×10^5 magnification, followed by analyses using a commercial statistic software.

The catalytic activity of Ag−Pd bimetallic nanoparticles in TiO_2 thin film was evaluated by the rate of hydrogenation of methyl acrylate in ethanol at 30 °C under 1 atm of hydrogen. The Ag−Pd bimetallic nanoparticle (2.0×10^{-7} mol of palladium) and ethanol (19 mL) were placed in a flask, the atmosphere of which had been replaced in advance with hydrogen of one atmospheric pressure. The mixture was stirred for 2 h at 30 °C to activate the catalyst. Then, an ethanol solution (1 mL) containing 0.5 mmol of methyl acrylate was added to the mixture, keeping the total pressure at 1 atm. The reaction was traced by hydrogen uptake with a temperature-controlled gas buret. The rate of hydrogenation was calculated from the initial slope of the hydrogen uptake.[7] For comparison, Pd monometallic nanoparticles embedded in a TiO_2 thin

(10) Toshima, N. *Macromol. Symp.* **2000**, *156*, 45−52.
(11) Arnold, G. W. *J. Appl. Phys.* **1975**, *46*, 4466−4473.
(12) Tanahashi, I.; Manabe, Y.; Tohda, T.; Sasaki, S.; Nakamura, A. *J. Appl. Phys.* **1996**, *79*, 1244−1249.
(13) (a) Yazawa, T.; Kadono, K.; Tanaka, H.; Sakaguchi, T.; Tsubota, S.; Kuraoka, K.; Miya, M. *J. Non-Cryst. Solids* **1994**, *170*, 105−108; (b) Innocenzi, P.; Brusatin, G.; Martucci, A.; Urabe, K. *Thin Solid Films* **1996**, *279*, 23−28.
(14) Yonezawa, T.; Matsune, H.; Kunitake, T. *Chem. Mater.* **1999**, *11*, 33−35.
(15) Joly, S.; Kane, R.; Radzilowski, L.; Wang, T.; Wu, A.; Cohen, R. E.; Thomas, E. L.; Rubner, M. F. *Langmuir* **2000**, *16*, 1354−1359.
(16) He, J.; Ichinose, I.; Fujikawa, S.; Kunitake, T.; Nakao, A. *Chem. Mater.* **2002**, *14*, 3493−3500.
(17) He, J.; Ichinose, I.; Kunitake, T.; Nakao, A. *Langmuir* **2002**, *18*, 10 005−10 010.
(18) He, J.; Ichinose, I.; Fujikawa, S.; Kunitake, T.; Nakao, A. *Chem. Commun.* **2002**, 1910−1911.

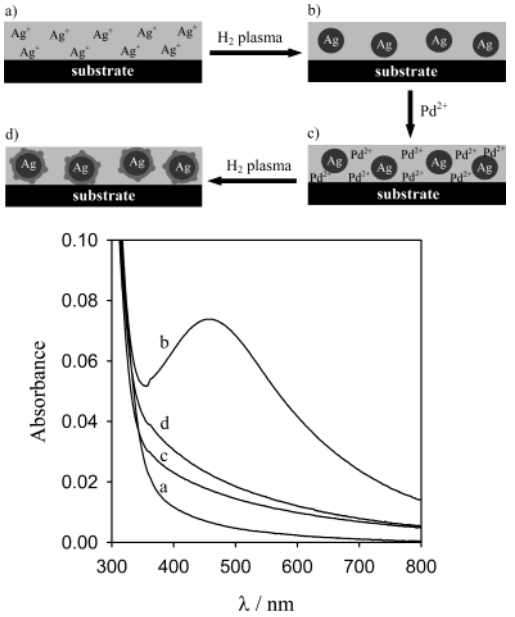

Figure 1. Preparation of Pd-on-Ag core−shell bimetallic nanoparticles in TiO_2 thin film by sequential incorporation/reduction of Ag^+ and Pd^{2+} ions (up) and corresponding UV−visible spectra of the thin film (below) (a) after 4 h immersion in aqueous $AgNO_3$ (10 mM); (b) after exposure to H_2 plasma of 10 w for 150 s; (c) after 4 h immersion in aqueous $Pd(NO_3)_2$ (10 mM); and (d) after exposure to H_2 plasma of 10 w for 5 s.

film were also prepared. The catalytic activities of these films and commercial Pd black (Wako Pure Chem) were evaluated in the same way.

Results and Discussion

Preparation of Pd-on-Ag Bimetallic Nanoparticles in TiO_2-Gel Films. The combination of silver and palladium was selected as the first bimetallic example, because of the ease of characterization. Nanosized metallic silver shows strong surface plasmon absorption, whereas nanosized palladium metal only shows a broad absorption tail in the same region. This difference facilitates characterization of bimetallic nanoparticles by UV−vis spectroscopy.

Ultrathin films were assembled on quartz substrates from a mixture of $Ti(O\textit{n}Bu)_4$ (100 mM) and $Mg(OEt)_2$ (10 mM) in 2-ethoxyethanol by the surface sol−gel process. After eight cycles of the process, the film thickness reached ca. 20 nm, as estimated by frequency changes of quartz crystal microbalance (QCM) (USI, Fukuoka, Japan). The template Mg^{2+} ions were removed from the film by treatments with aqueous HCl (pH 4) and aqueous NaOH (pH 10), creating Na^+ ion-exchange sites in the film. The Ag^+ ion was then incorporated by immersing in aqueous $AgNO_3$, and this Ag^+-doped thin film gives a UV−vis spectrum that shows an absorption tail in the range of 300−800 nm (Figure 1a). When it was exposed to low-temperature H_2 plasma, an absorption peak appeared at 462 nm, which is undoubtedly derived from surface plasmon resonance of Ag nanoparticles (Figure 1b). Subsequent immersion of the film in aqueous $Pd(NO_3)_2$ (10 mM) for 4 h caused complete disappearance of the surface plasmon peak, probably as a result of Pd^{2+} adsorption on the Ag nanoparticle (Figure 1c). When this film was again exposed to H_2 plasma, an absorbance increase was observed at 320−800 nm (Figure 1d), in consistence with the formation of Pd nanoparticles.[17] It is known that the intensity of Au plasmon band for Au-core/Pd-shell bimetallic nanoparticles decreases with increasing Pd/Au ratio and that the band completely disappears at the Pd fraction over 60%.[5] Very recently, it was found that physical mixing of polymer-protected Ag and Rh monometallic nanoparticles resulted in Ag-core/Rh-shell bimetallic nanoparticles, causing disappearance of the surface plasmon band of the silver nanoparticle.[19] We can conclude that Pd-on-Ag bimetallic nanoparticles are formed in the current procedure, from the observed variation of the surface plasmon peak.

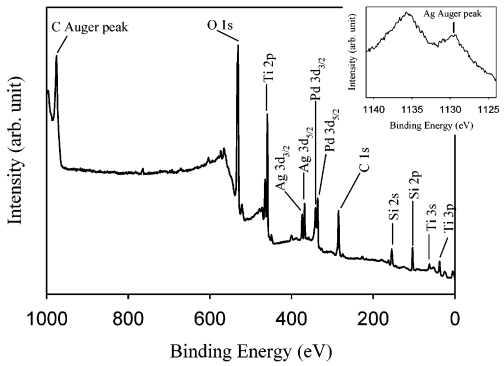

Figure 2. XPS spectrum of the specimen of Figure 1d: Pd-on-Ag core−shell bimetallic nanoparticles in TiO_2-gel film.

Formation of the core−shell bimetallic structure was, in fact, confirmed by X-ray photoelectron spectroscopy (XPS) and TEM observation. The specimen of Figure 1d was cleaved into two pieces, one for XPS measurements and the other for TEM observation. As shown in Figure 2, XPS peaks were observed at 459.2 eV (Ti $2p_{3/2}$, matrix), 368 eV (Ag $3d_{5/2}$), and 335.8 eV (Pd $3d_{5/2}$). The Auger peak of Ag metal was found at 1129.3 eV (Figure 2, insert). The Ag kinetic energy (MNN) was estimated to be 356.9 eV. The modified Auger parameter ($\alpha = E_K(\text{MNN}) + E_B(3d_{5/2})$) was then calculated to be 725.3 eV, in agreement with the reported value of metallic silver ($\alpha = E_K(\text{MNN})$ (357.9 eV) $+ E_B(3d_{5/2})$ (368.2 eV) $= 726.1$ eV).[20] Therefore, silver exists in its metallic state in the thin film. The Pd $3d_{5/2}$ peak at 335.8 eV is also attributed to metallic palladium. However, deviation of the binding energy of Pd $3d_{5/2}$ was noticed from those of pure metallic Pd (335.2 eV)[21] and Pd in TiO_2 film (336.3 eV).[17] The peak shift of Pd in TiO_2 matrix relative to that of pure Pd metal is attributed to the electron withdrawing effect of the surrounding TiO_2 matrix. In contrast, the shift of the binding energy of monometallic Pd in TiO_2 (336.3 eV) to a lower value (335.8 eV) in the present Pd-on-Ag bimetallic nanoparticle is attributable to an additional electron donating effect from core Ag atom to shell Pd atom. The atomic ratio of Pd to Ag was determined to be 2.2 from their peak areas after correction of sensitivity factors, and this ratio is similar to that observed in the literature for Au-core/Pd-shell bimetallic nanoparticles.[5,6]

The subsequent TEM observation gave a more direct view of the morphology of the bimetallic nanoparticle. The nanoparticle-containing TiO_2 film (Figure 1d) was scratched off from its quartz substrate in 2-ethoxyethanol, transferred to a 200-mesh, carbon-coated copper grid by a dispenser, allowed to dry,

(19) Hirakawa, K.; Toshima, N. *Chem. Lett.* **2003**, *32*, 78−79.
(20) Moulder, J. F.; Stickle, W. F.; Sobol, P. E.; Bomben, K. D. In *Handbook of X-ray Photoelectron Spectroscopy*; Chastain, J., Ed.; Perkin-Elmer Corpration.
(21) Lide, D. R.; Ed. *CRC Handbook of Chemistry and Physics*, 81st Ed.; CRC Press LLC: Boca Raton, FL,2000, pp 10−203.

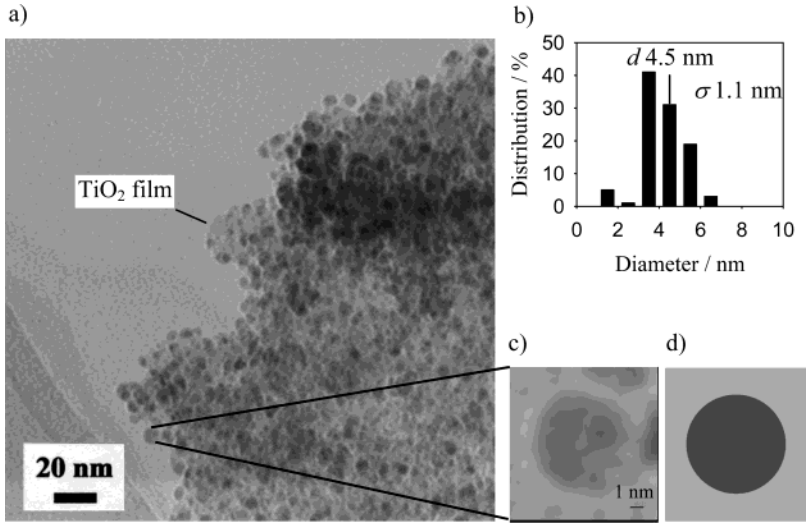

Figure 3. TEM image (a), histogram (b), and magnified image (c) of Ag monometallic nanoparticles in TiO_2-gel film, and (d) cross-section model.

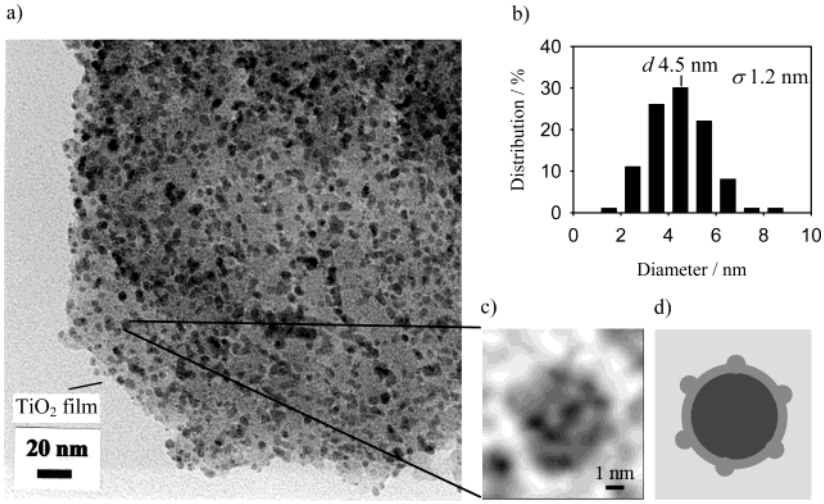

Figure 4. TEM image (a), histogram (b), and magnified image (c) of Pd-on-Ag core−shell bimetallic nanoparticles in TiO_2-gel film prepared by sequential incorporation/reduction of Ag^+ and Pd^{2+} ions, and (d) simplified cross-section model.

and then observed by TEM. The monometallic Ag nanoparticle of 4.5 nm in diameter and 1.1 nm in standard deviation gives a rather uniform spherical particle as shown by a TEM image of Figure 3. In contrast, a TEM image of the bimetallic nanoparticle is more irregular (Figure 4a). Both spherical and elongated nanoparticles exist in the thin TiO_2 matrix. Figure 4b gives a histogram of 100 nanoparticles that were sampled as evenly as possible in the whole area of the TEM picture. A symmetrical size distribution is noted with mean diameter of 4.5 nm and standard deviation of 1.2 nm. When the nanoparticle is observed at an enhanced magnification, dot-like structures of 1.0−1.5 nm are noticed on the surface of the bimetallic nanoparticle (Figure 4c). The outer shell layer appears not uniform in thickness, and Pd clusters may be formed on top of the Pd shell, as schematically illustrated in Figure 4d. Such a morphology is expected to have a very high Pd surface area and, correspondingly, extremely high catalytic activities.[22,23]

Assuming that the nanoparticle is spherical and consists of the ideal core−shell structure, we can make rough estimates of the atomic distribution in the Pd-on-Ag bimetallic and Ag monometallic nanoparticles from their radii, densities, atomic weights and atomic ratio (in the case of bimetallic nanoparticle). As shown in Figure 5a, the following equation exists for a monometallic nanoparticle

$$N = \frac{4}{3}\pi R^3 d / \frac{\mathrm{AW}}{N_\mathrm{A}} \qquad (1)$$

where N is the number of atoms in the nanoparticle, R is its radius, d is the metal bulk density (10.5 g/cm^3 for silver), AW is the metal atomic weight, N_A is the Avogadro constant. Thus, there are ca. 3.3×10^3 Ag atoms in the 4.5 nm (R) Ag nanoparticle.

In the case of the bimetallic nanoparticle (Figure 5b), the shell (metal 1) to core (metal 2) atomic ratio (N_1/N_2) is expressed as follows

$$\frac{N_1}{N_2} = \left(\frac{4}{3}\pi(R_1^3 - R_2^3)d_1 / \frac{\mathrm{AW}_1}{N_\mathrm{A}}\right) / \left(\frac{4}{3}\pi R_2^3 d_2 / \frac{\mathrm{AW}_2}{N_\mathrm{A}}\right) \qquad (2)$$

where R_1 and R_2 are the radii of bimetallic nanoparticle and its core, d_1 and d_2 are the bulk densities of shell and core metals,

(22) Nishihata, Y.; Mizuki, J.; Akao, T.; Tanaka, H.; Uenishi, M.; Kimura, M.; Okamoto, T.; Hamada, N. *Nature* **2002**, *418*, 164−167.
(23) Hermans, S.; Raja, R.; Thomas, J. M.; Johnson, B. F. G.; Sankar, G.; Gleeson, D. *Angew. Chem., Int. Ed. Engl.* **2001**, *40*, 1211−1215.

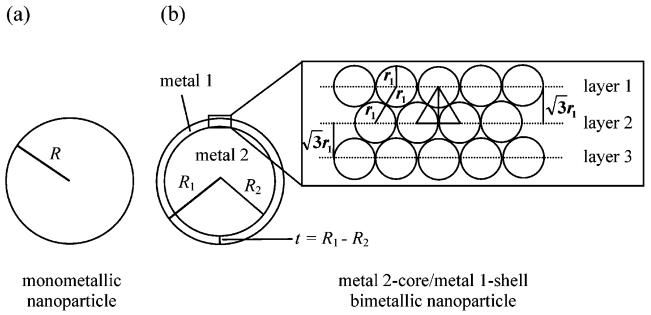

Figure 5. Illustration of ideal monometallic (a) and core−shell bimetallic (b) nanopartcles. R, R_1, and R_2 are radii of monometallic nanoparticle, bimetallic nanoparticle and its core; r_1 is atomic radius of shell metal.

AW_1 and AW_2 are the atomic weights of shell and core metals, respectively. For the Pd-on-Ag nanoparticle, d_1 (Pd) and d_2 (Ag) are 12.0 and 10.5 g/cm^3, respectively, and $N_{1(Pd)}/N_{2(Ag)}$ is 2.2 (from XPS data). Therefore, we can calculate from eq 2 the diameter of the interior core ($2R_2$) as 3.2 nm, and this gives 9.7×10^2 Ag atoms from eq 1. Thus, the exterior shell has a thickness ($t = R_1 - R_2$) of 0.7 nm and contains 2.1×10^3 Pd atoms. From the Pd atomic radius (r_1) of 0.14 nm, the thickness of each atomic layer is ca. $\sqrt{3}r_1 = 0.24$ nm, and, therefore, the shell roughly consists of 3 Pd atomic layers (Figure 5b). It is clear from the TEM image that the bimetallic nanoparticle does not assume an idealized core−shell morphology. A more realistic model is given as Figure 4d. This model is represented by small Pd particles (d, 1.0−1.5 nm) attached onto the surface of a larger (d ~3.6 nm) Ag particle. The remaining surface should also be covered with Pd atomic layers, as suggested by the complete disappearance of the Ag plasmon band after deposition of Pd (Figure 1). A surfactant stabilized Au−Pd bimetallic nanoparticle with similar spectrum changes in synthesis was confirmed by high resolution TEM to have an Au core fully covered by a Pd shell.[6] The current model will increase the number of exposed Pd atoms, but a precise model building is not possible from the available data.

Nanoparticles Prepared by the Reversed Order of Incorporation. It is important to confirm the composition and morphology of the bimetallic particle for which incorporation of the two metals is reversed. Thus, Pd^{2+} ion was introduced into a TiO_2-gel film prior to Ag^+ incorporation under otherwise the identical conditions. After 4 h immersion in aqueous $Pd(NO_3)_2$ (10 mM) and exposure to H_2 plasma, the Mg^{2+}-templated thin film showed a spectral increase due to formation of Pd nanoparticles (Figure 6a and b). Subsequent immersion in aqueous $AgNO_3$ (10 mM) and exposure to H_2 plasma resulted in formation of metallic Ag nanoparticles, as indicated by appearance of a Ag surface plasmon peak (Figure 6d). The peak position of the plasmon band was estimated to be at 421 nm by subtracting Figure 6b from Figure 6d. This surface plasmon peak is blue-shifted and its intensity dramatically decreases compared with that found in Figure 1b, indicating that the Ag nanoparticle may be much smaller than those observed in Figure 3a. XPS measurements on the sample showed the Pd $3d_{5/2}$ peak at 336.52 eV, which is identical to that of metallic Pd in TiO_2 matrix. Thus, Pd and Ag elements are apparently not interacting within nanoparticles. This suggests that Ag-on-Pd nanoparticles of core−shell type are not obtained, contrary to our expectation, i.e., isolated Pd and Ag metallic nanoparticles are formed. It

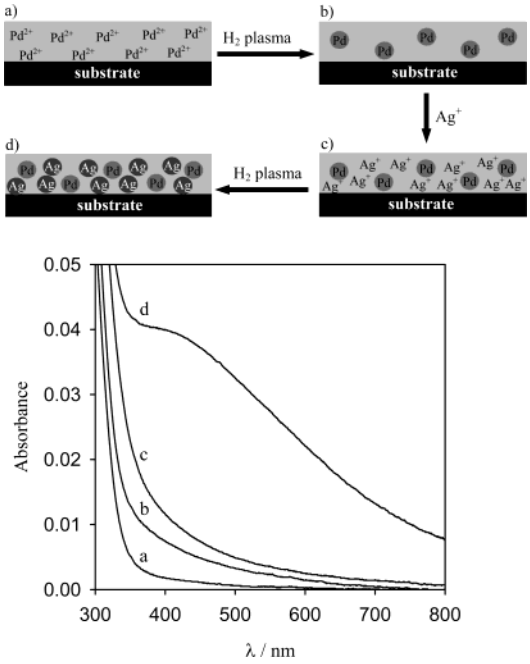

Figure 6. Preparation of nanoparticles in TiO_2 thin film by sequential incorporation/reduction of Pd^{2+} and Ag^+ ions (up) and corresponding UV−vis spectra of the thin film (below) (a) after 4 h immersion in aqueous $Pd(NO_3)_2$ (10 mM); (b) after exposure to H_2 plasma of 10 w for 5 s; (c) after 4 h immersion in aqueous $AgNO_3$ (10 mM); and (d) after exposure to H_2 plasma of 10 w for 450 s.

may not be surprising if we take into account the redox potentials of the two elements involved. Ag has a lower redox potential (0.7996 V) than Pd (0.951 V), leading to the difficulty of forming an Ag-on-Pd nanoparticle. As a similar situation, a successive reduction of Au^{3+} (1.498 V) and Pd^{2+} (0.951 V) in solution was reported to give a mixture of Au and Pd individual clusters rather than Pd-on-Au bimetallic particles.[24] TEM images of this sample show very small nanoparticles, with mean diameter of 1.6 nm and standard deviation of 0.38 nm (Figure 7). They must be composed of both of Pd and Ag metallic nanoparticles, but they are not distinguishable by TEM. XPS results showed that a large amount of Ag atom was incorporated: Pd/Ag ratio is 0.17. It is presumed that most of the Ag atoms underwent aggregation among themselves. It is estimated from this ratio that the nanoparticles are composed of 85% Ag nanoparticles and 15% Pd nanoparticles.

Catalytic Activity of Pd-on-Ag Bimetallic Nanoparticles. The catalytic activity of the Pd-on-Ag bimetallic nanoparticle in TiO_2 thin film was evaluated for hydrogenation of methyl acrylate, and compared with that of Pd monometallic nanoparticle (average diameter, 5.0 ± 1.9 nm) in TiO_2 film and commercial Pd black (Wako Pure Chem). Under identical conditions, the catalytic activity of the commercial palladium black, as estimated from the initial rate, was measured to be 0.0045 mol·H_2 mol·Pd^{-1} s^{-1}.[25] In contrast, the catalytic activity of the monometallic Pd nanoparticle was estimated to be 1.05 mol·H_2 mol·Pd^{-1} s^{-1}, 233 times as large as that of the commercial palladium black. In the latter, considerable aggregation of large Pd particles is observed. Thus, the higher

(24) Harada M.; Asakura, K.; Toshima, N. *J. Phys. Chem.* **1993**, *97*, 5103−5114.
(25) Toshima, N.; Shiraishi, Y.; Teranishi, T.; Miyake, M.; Tominaga, T.; Watanabe, H.; Brijoux, W.; Bönnemann, H.; Schmid, G. *Appl. Organomet. Chem.* **2001**, *15*, 178−196.

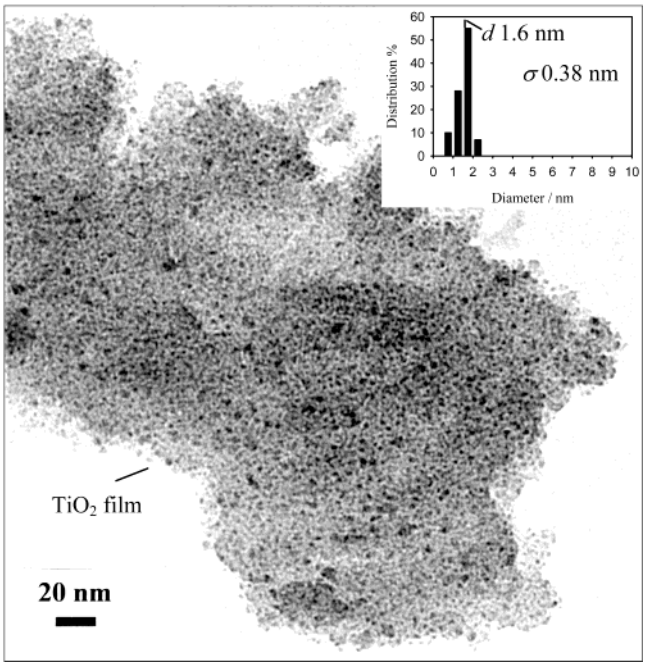

Figure 7. TEM image of Pd and Ag nanoparticles in TiO_2-gel film prepared by sequential incorporation/reduction of Pd^{2+} and Ag^+ ions.

catalytic activity of the Pd nanoparticle is attributable at least partially to its much smaller size and the resulting enhanced surface area. The TiO_2 matrix might provide an interfacial area that could promote the catalytic activity of Pd atom, as recently discussed by others.[26] When the Pd-on-Ag bimetallic nanoparticle was tested, a linear hydrogen uptake was observed up to ca. 14 cm^3 in ca. 40 min, where the hydrogen uptake was almost saturated. The saturated hydrogen uptake (ca. 14 cm^3) was in reasonable agreement with that (12.4 cm^3) estimated from hydrogenation of the C=C bond, but not of the C=O bond in methyl acrylate.[27] The catalytic activity was estimated to be 1.65 mol·H_2 mol·Pd^{-1} s^{-1}. It is 367 times as large as that of the commercial palladium black and 1.6 times as large as that of the monometallic Pd nanoparticle.

It is interesting to estimate the fraction of Pd atoms that are located on the outmost surface. Again by assuming that the Pd monometallic nanoparticle is spherical (Figure 5a), the fraction of surface Pd atoms is calculated as ca. 24%,[28] i.e., ca. 76% Pd atoms are located in the interior of nanoparticle and could not be directly accessed by reactants. On the other hand, Pd atom exists as 3 atomic layers on the Ag core for the Pd-on-Ag nanoparticle. Among the latter Pd atoms, ca. 42% are located on the particle surface.[29] In a more realistic model of Figure 4d, this value may be even higher. Thus, the ratio of the surface Pd atoms in the bimetallic Ag-core/Pd-shell nanoparticle and the Pd monometallic nanoparticle is 1.7. This is a striking agreement with the ratio of their catalytic activities (1.6). We

(26) (a) Cho, A. *Science* **2003**, *299*, 1684−1685; (b) Bell, A. T. *Science* **2003**, *299*, 1688−1691; (c) Rolison, D. R. *Science* **2003**, *299*, 1698−1701.

(27) The Boyle's law for ideal gas: $PV = nRT$, where P is the pressure, V is the volume, T is the temperature, n is the amount of substance in moles, R is the gas constant. In the current experiment, $P = 1$ atm, $T = 303$ K, $n = 5 \times 10^{-4}$ mol, $R = 82.0578$ atm cm^3 K^{-1} mol^{-1}.

(28) The number of surface Pd atoms: $N_S = 4\pi(R - r)^2 \times 0.90/\pi r^2 = 4(R - r)^2/r^2 \times 0.90$, the total number of Pd atoms: $N_T = 4/3\ \pi R^3 \times 0.74/(4/3\ \pi r^3) = R^3/r^3 \times 0.74$, wherein R is the radius of nanoparticle (2.5 nm), r is that of atom (0.14 nm), 0.90 and 0.74 are the two and three-dimensional packing coefficients, respectively. Thus the ratio N_S/N_T can be estimated.

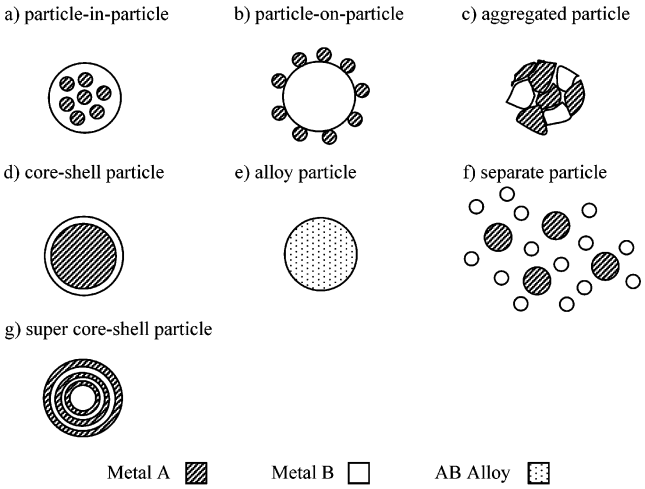

Figure 8. Representative morphologies of bimetallic nanoparticles.

can conclude from these considerations that the observed higher catalytic activity of the Pd-on-Ag nanoparticle is attributed mainly to the large fraction of surface Pd atoms.

Possible Morphologies of Bimetallic Nanoparticles. It is appropriate at this point to summarize representative morphological variations of bimetallic nanoparticles, as given in Figure 8. Although Figure 8a is the morphology of metal A particles included in a metal B particle, Figure 8b shows that of metal A particles attached on the surface of a metal B particle. In Figure 8c, a particle is formed as a result of aggregation of A and B sub-particles (domains). Core−shell and alloy morphologies are displayed in Figure 8d and e, respectively. Separate particles of metal A and metal B (Figure 8f) are also an important member of the bimetallic nanoparticle. Further variations are possible by combination or repetition of these representative structures, and by exchanging metal A and metal B in the first four cases. Crystallinity or the lack of it leads to an additional variety. A super core−shell structure of onion-like morphology is conceivable based on alternate layering of two metals (Figure 8g). In the present example, an irregular core−shell morphology was formed for Pd-on-Ag particles, and this may be conceived as a mixed structure of b and d. On the other hand, separate particles (structure f) appear to be dominant for the Ag-on-Pd system.

These varied morphologies may be categorized in terms of continuity of a metal phase. Thus, in the case of particle-in-particle, the outer particle constitutes a continuous phase, and the inner particles are discontinuous. The particle-on-particle, in contrast, is made of discontinuous outer particles and a continuous inner particle. Both of the two metal phases can be discontinuous in the aggregated bimetallic particle, whereas both metal phases are continuous in the core−shell structure. The alloy particle, of course, provides a new phase that is different from either of the two metal phases. The electronic property of the bimetallic particle would be altered extensively, depending on size, atomic order and continuity of the metal phase. How

(29) The numbers of the surface, sub- and sub, subsurface Pd atoms: $N_{S_1} = 4\pi(R_1 - r_1)^2 \times 0.90/\pi r_1^2$, $N_{S_2} = 4\pi(R_1 - r_1 - \sqrt{3}r_1)^2 \times 0.90/\pi r_1^2$, $N_{S_3} = 4\pi(R_1 - r_1 - \sqrt{3}r_1 - \sqrt{3}r_1)^2 \times 0.90/\pi r_1^2$ (see Figure 5b), R_1 and r_1 are the radii of the Pd-on-Ag nanoparticle (2.25 nm) and Pd atom (0.14 nm). Thus, the fraction of surface atoms is: $N_{S_1}/(N_{S_1} + N_{S_2} + N_{S_3}) = (R_1 - r_1)^2/[(R_1 - r_1)^2 + (R_1 - r_1 - \sqrt{3}r_1)^2 + (R_1 - r_1 - \sqrt{3}\ r_1 - \sqrt{3}r_1)^2]$.

the quantized electronic states of the two metals interact in bimetallic nanoparticles is a rich source of new physical and chemical properties. Multi-metallic nanoparticles would also lead to super-active catalysts for petrochemicals and fuel cells. Bimetallic and multi-metallic nanoparticles of varied morphologies are expected to have unique properties that are quite distinct from those of the corresponding monometallic nanoparticles.

Conclusions

Bimetallic and multi-metallic nanoparticles belong to a class of the highly important nanomaterials that are largely unexplored. Apart from their quantum size effects, possible combinations of metallic elements in nanoparticles can be numerous, and electronic and quantum interactions among component metals may produce totally new physical and chemical properties.[4] Variation of particle morphology is another rich source of tailoring their physicochemical properties.[30] These nanoparticles are in many cases not stable without protective organic groups, which can again exert strong influences on their multimetallic properties.

In view of such structural complications and rich functional possibilities, it is much desired to find a method for facile preparation of multi-metallic nanoparticles. We described in the present study a simple preparative method of bimetallic nanoparticles in the TiO_2 ultrathin film. There are several unique features that deserve special comments. One is the generality and simplicity of this preparative method. Metallic elements are incorporated into thin films as a result of ion-exchange and reduction. This process is simple, and the repetition of this process can readily produce bimetallic nanoparticles in the desired order of incorporation. The ambient preparative conditions are energy-saving, and expensive experimental setup is not required.

A second notable feature is that the resulting metallic nanoparticle is stabilized by metal oxide networks, without relying on organic ligand molecules. Oxygen atoms in the network must stabilize bare metal ions, in a way similar to crown ethers, in which coordinating oxygen atoms are juxtaposed toward central metal ions. After reduction, such coordination is insufficient to maintain isolated metal atoms in the TiO_2 matrix, because of their high mobility and reactivity. These metal atoms tend to coalescence, forming metal nanoparticles. With the increase in particle size, the mobility and reactivity are lowered compared with those of the metal atom, and the metal nanoparticle will be ultimately stabilized by a strong bonding interaction between the outmost orbitals of its surface atoms and the surrounding oxygen atoms of the TiO_2 matrix, as demonstrated for a Ti metal cluster.[31] The absence of the organic ligand is related to many advantages in practical applications. A third feature is that metallic nanoparticles are produced directly in solid matrix. Many practical uses of nanoparticles are made possible only in solid supports. This requirement is met without additional procedures in the current system. The catalytic experiment suggests that small reacting molecules can penetrate to the catalytic site through the metal oxide network. It is important to point out that we are dealing very thin, porous films where molecular diffusion cannot be rate-limiting.

These outstanding features will bring about a new stage of development in metallic nanoparticle research. For instance, the efficient use of noble metals is indispensable for development of practical fuel cells for automobiles. We may adopt the flexible design of bimetallic nanoparticles for this purpose. More elaborate, multi-metallic systems are readily available for the purpose of examining further unexplored possibilities.

Acknowledgment. We thank Dr. M. Shimizu for discussion in absorption spectroscopy (FRS, RIKEN) and Dr. Onoue (Kyoritsu Chemical/Presto, JST/FRS, RIKEN) for discussion in structural estimation. J. He is grateful to Japan Science and Technology Corporation (JST) for a STA fellowship.

JA035970B

(30) Pileni, M. P. *Nat. Mater.* **2003**, *2*, 145−150.

(31) Franke, R.; Rothe, J.; Pollmann, J.; Hormes, J.; Bönnemann, H.; Brijoux, W.; Hindenburg, Th. *J. Am. Chem. Soc.* **1996**, *118*, 12 090−12 097.